

Article

Variation in Feedstock Wood Chemistry Strongly Influences Biochar Liming Potential

Sossina Gezahegn^{1,*}, Mohini Sain^{1,2} and Sean C. Thomas³ 

¹ Centre for Biocomposites and Biomaterials Processing, Faculty of Forestry, University of Toronto, Toronto, ON M5S 3B3, Canada; m.sain@utoronto.ca

² Department of Mechanical and Industrial Engineering, University of Toronto, 5 King's College Road, Toronto, ON M5S 3G8, Canada

³ Faculty of Forestry, University of Toronto, Earth Sciences Building, 33 Willcocks Street, Toronto, ON M5S 3B3, Canada; sc.thomas@utoronto.ca

* Correspondence: s.gezahegn@mail.utoronto.ca

Received: 4 February 2019; Accepted: 27 March 2019; Published: 3 April 2019



Abstract: Chars intended for use as soil amendment (“biochars”) vary greatly in their chemical and physical properties. In the present study, 19 Canadian temperate wood feedstocks were charred across a range of pyrolysis temperatures from 300–700 °C. The resulting 95 biochars were tested for their physio-chemical properties and liming capacity. Data indicated increasing base cation concentrations including Ca, Mg, and K (elements that characteristically form liming compounds, i.e., carbonates) as pyrolysis temperature increased. Acidic surface functional groups were analyzed with modified Boehm titration: Carboxylic and lactonic functional group concentrations decreased and phenolic group concentration increased with pyrolysis temperature. Functional group composition also varied greatly with feedstock: In particular, conifer-derived biochars produced at pyrolysis temperatures <500 °C showed much higher carboxylic and lactonic functional group concentrations than did angiosperm-derived biochars. Liming capacity was assessed using soil incubation experiments and was positively related to biochar pH. Both acidic surface functional group concentration and nutrient element concentration influenced biochar pH: we developed a non-linear functional relationship that predicts biochar pH from the ratio of carboxylic to phenolic moieties, and concentrations of Ca and K. Biochar’s liming components that are inherited from feedstock and predictably modified by pyrolysis temperature provide a basis for optimizing the production of biochar with desired pH and liming characteristics.

Keywords: acidic groups; cations; char; pH; pyrolysis

1. Introduction

Chars are ubiquitous geosorbents that are created from incomplete pyrolysis of carbon-rich biomass in the presence of little or no oxygen. Chars applied as a soil amendment have been labeled “biochars” [1]: biochars sequester carbon in soils and their carbon is generally much more stable than carbon in the original biomass. Biochars produced at moderate to high temperatures are very resistant to microbial decomposition, and therefore can be retained in soils for mean residence times of hundreds to thousands of years [2]. In contrast, composts generally mineralize rapidly and therefore frequent application is generally needed to maintain sufficient nutrient content, cation exchange capacity, and C content [3]. In comparison to other forms of organic matter used as soil amendments, biochars also reduce waste volume, and reduces risks from pathogens, heavy metals [4], and organic pollutants [5]. Biochars have commonly been produced from wood wastes, grasses, crop residues, and animal manure feedstocks [6].

Physical and chemical properties of biochars vary greatly, potentially allowing one to produce a suitable biochar for specific applications by optimizing feedstock selection and pyrolysis conditions [6,7]. During pyrolysis, the electron cloud arrangement in the carbon skeleton varies as a function of the quantity of thermally modified carbon layers [8], resulting in significant differences in biochar properties. Biochar structure contains mostly amorphous and some crystalline parts (conjugated aromatic compounds) [9]; the latter increase with the highest treatment temperature (HTT) [10]. The biochar matrix also includes aromatic-aliphatic groups, residual volatiles, and inorganic ashes [11] with varying morphologies of voids, cracks, and pores (at micro-, meso-, and macro-scales) [12]. Pyrolysis temperature strongly affects the molecular architecture of biochar in terms of surface area, pore number, and pore size [13], as well as surface area functional groups [14]. Prior studies have suggested a linear response of biochar pH to HTT, but well-resolved temperature response curves are few (for example, see References [15,16]). In all cases, higher aromaticity is expected at higher pyrolysis temperatures [17], but feedstocks may vary in temperature response pattern. Particle size can influence biochar properties since larger particles resist the escape of primary products during pyrolysis compared to smaller biomass particles [18]. In addition, biochar yield commonly increases with increasing particle size [19].

Biochars generally have a substantial liming capacity, due in large part to mineral content carried over from feedstock [1], which makes them a possible substitute for liming agents such as dolomitic limestone or aglime. The addition of biochar (with a typical pH of 8–9) to acidic soils generally results in increased soil pH and a concomitant decrease in the mobility of cationic metal ions. This occurs due to the competition of H^+ ions and metal ions for cation exchange sites on the biochar surface and the liming effect on the soil matrix [20]; as with geological liming materials, the main chemical mechanism for liming involves the formation of carbonates [21]. Positive effects of biochar on crop growth and yield are most pronounced on acid soils [22], suggesting the importance of liming effects. Liming is also of importance in biochar mitigation of heavy metal bioavailability: the application of biochar to alkaline or neutral soils does not result in a significant reduction in metal mobility, suggesting that the reduction in metal mobility is not due to biochar sorption, but rather to liming effects [20,23,24]. Biochar's pH increases as acidic surface functional groups are lost during pyrolysis and replaced by neutral or basic fused aromatic moieties [25]. Alkaline elements such as Mg, Ca, and K may also increase the pH in biochars if they are abundant in the feedstock [26]. In addition to effects on metal mobility, direct nutrient release (PO_4^{3-} , NH_4^+ , Mg^{2+} , K^+ , and Ca^{2+}) from biochar is also strongly pH dependent [27].

The relative effects of biochar types and dosages on plant nutrient supply and responses have received considerable recent attention in the contexts of agriculture [7,28] and forestry [29,30]. A common theme in this body of research is high variability among biochars: some biochars strongly promote crop yields, some are neutral, and some are detrimental [6,7]. This variation provides a strong motivation for studies aimed at enhancing mechanistic understanding needed to produce optimized biochars for specific crop and soil systems [7]. Other critical soil properties—for example, nutrient and water retention and cation exchange capacity (CEC) [31]—are also strongly affected by biochar's porous structure and surface functional groups [32].

Wood chemistry is known to vary substantially among tree species, in terms both macromolecular constituents (cellulose, hemicellulose, and lignin) [33,34] and trace element concentrations [35]. However, surprisingly few data are available on variation in biochar properties among tree species, with few comparative studies in the literature presenting data from more than one wood species [14,29,36,37]. Hemicellulose and cellulose degrade at lower temperatures and earlier during pyrolysis than lignin [38,39]. Among common feedstocks, wood biomass contains the highest lignin content, though this varies substantially among tree species. Most conifers have higher lignin levels than do temperate hardwoods; however, data compilations indicate that hardwoods vary from 14%–48% lignin and conifers from 21%–38% lignin [33]. Lignin not only varies among tree species in terms of content, but also in terms of chemistry: angiosperm wood contains guaiacyl-syringyl

linkages, while conifer wood mainly contains guaiacyl structures with a lower proportion of sinapyl units [40]. Variation in the thermal stability of oxygen-containing functional groups of these structures strongly modifies lignin's thermal decomposition range [41]. Conifer lignins are more thermally stable, while angiosperm lignins are less stable and may provide lower char yields [39]. Variation in biochar properties among wood species is thus expected to be strongly influenced by variation in lignin content and chemistry. This variation is also likely to result in large differences in responses of char properties to pyrolysis temperature.

Canadian forestry provides a wide range of wood feedstocks potentially applicable to biochar production [42]. Boreal and temperate forests together cover 417 million hectares and form the basis for Canadian forest products industries [43]. Sawmill byproducts—in particular, sawdust, lower-value wood chips, and bark residues—are important potential feedstock sources. Heschel and Klose [44] refer to these homogenous forest byproducts as “high-quality feedstocks”. Lignin sludge from paper mills is another potential candidate feedstock [26]. By converting low-value or waste materials into biochar, the wood products industry could potentially both reduce environmental impacts and enhance product output and diversity. Quantification of variation in biochar physical and chemical properties is essential in assessing feedstock potential and in developing “designer” biochars for specific applications.

In the present study, we compare biochars derived from a broad range of common woods in Canada as potential biochar feedstocks, across a range of pyrolysis temperatures, focusing on physio-chemical parameters of importance to liming effects. We specifically address the following questions: (1) Is there a relationship between wood feedstock pH and the pH of the biochar produced? (2) How do concentrations of mineral nutrients and metals vary among biochars as a function of wood feedstock and pyrolysis temperature? (3) How does biochar pH increase with pyrolysis temperature, and does this relationship vary among wood feedstock species? (4) How do the concentrations of nutrient elements and acidic surface functional groups in char influence pH and liming capacity?

2. Materials and Methods

2.1. Feedstock and Biochar Preparation

Samples of 19 different woody feedstocks were collected: 15 of the feedstocks were supplied by Haliburton Forest and Wildlife Reserve, a privately owned forest in central Ontario, Canada (43° 13' N, 78° 35' W); feedstock samples for *Pseudotsuga menziesii* (Mirb.) Franco and *Tsuga canadensis* (L.) Carrière were supplied by Limberlost Forest and Nadrofsky Lumber, respectively, Huntsville, Ontario, Canada; and *Pinus resinosa* Sol ex. Aiton and *Pinus strobus* L. were supplied by Freymond Lumber, Bancroft, Ontario, Canada. All samples were sawdust with particle sizes of 63–4000 µm and were pyrolyzed with a laboratory-scale GSL-1100X programmable tube furnace (2.0" outer diameter, 1.85" inner diameter and 24" length quartz tube, and 3.5" length perforated stainless-steel sample container) after their moisture content was adjusted to 5%. All biochars were produced under a N₂ atmosphere and the final temperatures were held for 1 h. Charring temperatures were raised at rates of 10, 13, 17, 20, and 23 °C/min to 300, 400, 500, 600, and 700 °C, respectively. Following pyrolysis, samples were allowed to cool to below 100 °C before exposure to oxygen. Supplemental Table S1 summarizes the feedstock and biochar samples used. Both feedstocks and biochars were placed in airtight containers at 5 °C prior to analysis.

2.2. pH Measurement of Feedstock Biochar and Soil–Biochar Incubation

pH measurements were taken using an Oakton pH Meter with glass electrode. Prior to pH measurements, biochars were ground using a mortar and pestle. Biochar and feedstock samples were shaken in distilled water for 24 h in 0.15 g/6 mL and 0.8 g/10 mL quantities, respectively (feedstocks generally showed higher water sorption than biochar samples; the concentrations used reflected the minimum quantity of water necessary to obtain measurable liquid samples). All samples were then filtered (0.2 µm) and measured immediately.

The soil used in the incubation experiment was of the brunisolic order, with sandy texture from parent material of granite bedrock and a pre-treatment pH value of 5.3 (pH measured in 1 g/4 mL reverse osmosis water). This soil was collected from a shallow depth (<10 cm) in the Haliburton Forest and Wildlife Reserve (details on soil analysis are given in Sackett et al. [29]). Soil incubations were conducted with duplicate samples of biochar–soil mixtures (0.008 w/w ratio; 50 g soil) incubated at room temperature (~20 °C) for 18 days in 100 mL plastic cups. For soil incubation tests, the pH of the biochar–soil mixture was directly measured after stirring to homogenize the mixture. Temperatures were recorded at 1-h intervals throughout the incubation experiment (using a Logtag TRIX-8 temperature logger). Initially, 30 mL of deionized water was added to each soil–biochar mixture. Evaporated water was replaced every 3 days and before each pH measurement was taken.

2.3. Determination of Oxygen-Containing Surface Functional Groups by Boehm Titration

A modified Boehm titration was conducted following Laird et al. [45]. Briefly, prior to titration, all biochar samples were ground with a mortar and pestle. To remove acid-soluble ash components (carbonates, hydroxide, and oxides), ground biochars were treated with 1:50 biochar:solution (*w/v*) ratios. First, 0.05 M HCl was added to the biochars, which were then shaken for 24 h. Subsequently, the mixture was filtered and washed twice with 1 M CaCl₂ and four times with deionized water. The pre-treated samples were allowed to dry for 72 h at 50 °C. Dried samples (0.5 g) were shaken with 50 mL of 0.05 M Boehm reactants of NaOH, NaHCO₃, and Na₂CO₃ for 24 h. After a 24-h equilibration time, the mixtures were filtered and extracts were further treated with a sparge method [46]. Three 10-mL aliquots were taken from equilibrated extracts, and 0.05 M HCl was added at a 2:1 *v/v* ratio for both NaOH and NaHCO₃ and at a 3:1 *v/v* ratio for Na₂CO₃ extracts. Acidified samples were sparged with N₂ for approximately 2 h to remove or minimize CO₂ prior to titration. NaOH (0.05 M) was standardized with potassium hydrogen phthalate and used to back-titrate samples where blank values were subtracted. End points were determined using phenolphthalein as an indicator.

2.4. Spectroscopy

Spectroscopic analyses were used to corroborate results of Boehm titration for a subset of chars analyzed. Solid-state nuclear magnetic resonance (SSNMR) spectroscopy analyses were performed using a Bruker 700 MHz spectrometer. Both 1D ¹H FastMAS spectra and 1D {¹H} ¹³C cross-polarization (CP) MAS spectra were acquired on an Agilent DD2 700 MHz spectrometer with an Agilent 1.6-mm FastMAS NMR probe. Only *Pinus resinosa* wood samples pyrolyzed at 300, 500, and 700 °C were analyzed by SSNMR. Each sample was ground into a finer powder using a mortar and pestle. The samples were packed into 1.6 mm zirconia rotors for 1D ¹H and ¹³C NMR acquisition and processing.

Fourier-transform infrared (FTIR) spectroscopy was conducted using a Bruker spectrometer model Tensor 27 with a spectral resolution of 4 cm⁻¹ within the range of 4000 to 400 cm⁻¹. Prior to spectra acquisition, all samples were prepared into compressed pellets from a homogenized mixture of 0.2 g Potassium bromide (KBr) and 0.25% biochar ground using a mortar and pestle.

Inductively coupled plasma-atomic emission spectroscopy (ICP-AES) analyses were performed using a PerkinElmer Optima 7300 DV with axially viewed plasma. Samples were digested with 5 mL trace metal grade (69%–70%) nitric acid following the published wet digestion method of Enders and Lehmann, 2012 [47]. Then, 0.5 g of biochar was transferred to a digestion vessel and allowed to sit for 24 h prior to digestion. Sample tubes were covered with glass stoppers both prior to and during digestion. The digestion block was then pre-heated to 120 °C and sample tubes were heated for 4 h. After cooling, 65 mL of deionized water was added to each sample to reach 5% nitric acid concentration and filtered (0.45 μm) prior to ICP analysis.

2.5. Statistical Analysis

Species and temperature effects on char properties were initially tested by two-way analysis of variance (ANOVA), where individual determinations of properties were treated as replicates. In cases where only a single measurement of char properties was made, the analyses were a non-replicated design, and thus required the assumption of no species \times temperature interaction [48]. Differences in char properties between conifer and angiosperm species were also tested by one- and two-way ANOVA. Multiple linear regression was used to examine effects of feedstock properties on char properties. Non-linear least squares regression was used to fit alternative functions to relationships between pyrolysis temperature and char properties within a given species, using the nls() function in R. Where significant effects were found, the most parsimonious model was selected using an information theoretic approach [49] by minimum Akaike's information criterion (AICc, corrected for variable number). All statistical analyses were conducted using R version 3.1.2 [50].

3. Results

3.1. Effects of Pyrolysis Temperature and Species on Biochar pH

Biochar pH generally increased with increasing pyrolysis temperature across all species (Figure 1a). There were statistically significant effects of both temperature and species on biochar pH ($F = 354.4_{1,57}$ and $F = 6.5_{1,57}$, respectively; $p < 0.001$ in both cases). The relationship between temperature and biochar pH was approximately linear from 300–700 °C (a second-order polynomial term in the model was not significant). In addition, there were statistically significant differences among species in feedstock pH ($F = 6.9_{1,93}$; $p = 0.01$). Significant differences were also observed between the mean pH values for conifers and angiosperms, with higher values for both feedstocks and biochars found in angiosperms (feedstock pH: Conifers, 4.80 and angiosperms, 5.47; biochar pH: Conifers, 7.87 and angiosperms, 8.29 (Figure 1b)).

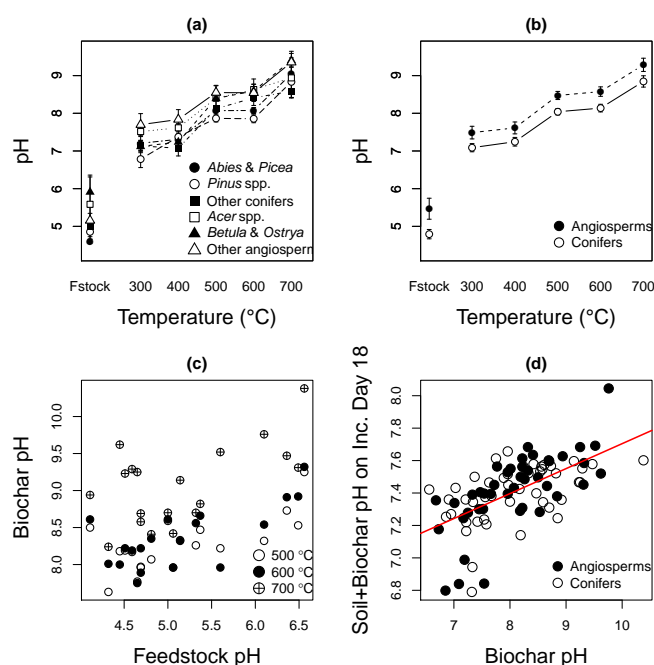


Figure 1. Biochar and feedstock pH as a function of temperature by taxonomic group (a) and grouped as conifers vs. angiosperms (b); biochar pH as a function of feedstock pH (c) and liming potential of biochar across five pyrolysis temperatures grouped by feedstock type; regression line drawn relating measured pH ($\text{pH of soil+biochar on incubation Day 18} = 0.15397 \times \text{Biochar pH} + 6.16463$) (d). All analyses are from 19 temperate tree species (conifer species ($n = 9$) and angiosperm species ($n = 10$)).

3.2. Feedstock and Biochar pH

Feedstock pH was correlated with biochar pH at 500, 600, and 700 °C pyrolysis temperatures ($r = 0.680$, $p = 0.001$; $r = 0.700$, $p < 0.001$; and $r = 0.610$, $p = 0.006$, respectively; Figure 1c), whereas at 300 and 400 °C, pH values did not show a significant correlation ($p > 0.05$). The overall relationship did not vary significantly among species ($F = 1.1$, $18, 76$; $p > 0.05$), but did differ between conifers and angiosperms considered as groups ($F = 5.5$, $2, 92$; $p = 0.01$).

3.3. Liming Potential of Biochar

Over the incubation period, soil–biochar mixtures generally showed an increase in pH values, and at day 18 and beyond, values plateaued. A strong correlation was found between biochar pH and the pH of incubated soil–biochar mixtures (at day 18: $r = 0.600$, $p < 0.001$). The relationship between biochar pH and incubated sample pH is shown in Figure 1d. There were statistically significant effects of both temperature and species on incubated soil–biochar sample pH ($F = 300.0$, $1, 51$ and $F = 9.1$, $18, 51$, respectively; $p < 0.001$ in both cases). The relationship between biochar pH and incubated soil pH differed between feedstock types, i.e., conifer vs. angiosperm ($F = 5.5$, $2, 92$; $p < 0.001$).

3.4. Elemental Analysis

As pyrolysis temperature increased, biochar samples showed an increase in concentration of several alkaline elements (Ca and Mg—occurring at the highest concentrations—as well as K, Fe, Mn, Na, and Zn); in all cases, feedstocks contained the lowest concentrations of each of these elements (Figure 2a–g). ANOVA results indicated that there were significant effects of both species and pyrolysis temperature on alkaline element and metal concentrations, with the following exceptions: No relationship was found between pyrolysis temperature and either Na or Zn concentration (Table 1). Higher mean element concentrations were generally observed for biochars of angiosperms as compared to conifers; this relationship was significant for K and Mg ($p < 0.001$), Na ($p < 0.01$), and Fe ($p < 0.05$) (Table 1).

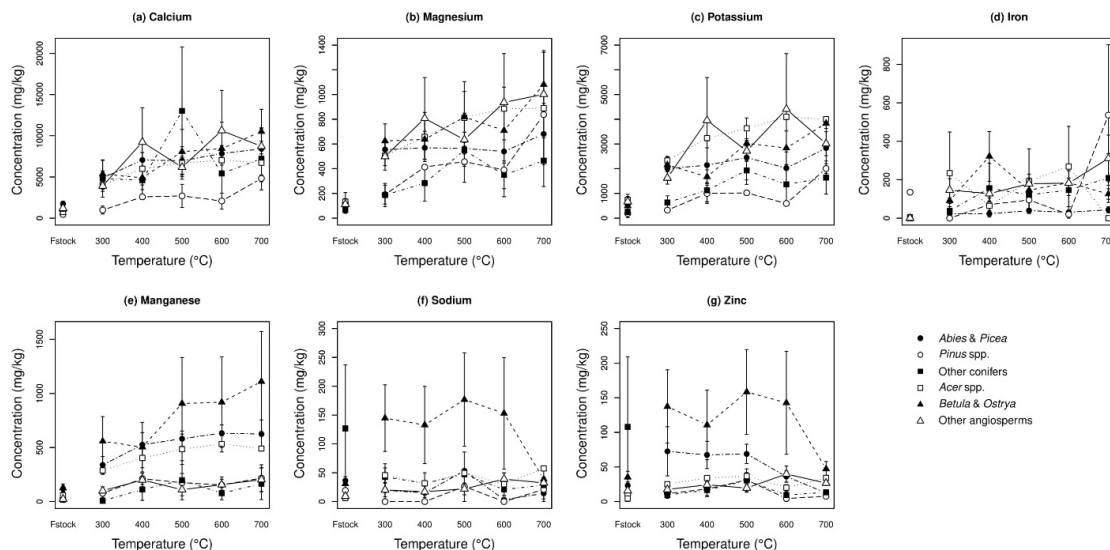


Figure 2. Inductively coupled plasma-atomic emission spectroscopy (ICP-AES) alkaline elements concentration plots of (a) Ca, (b) K, (c) Mg, (d) Fe, (e) Mn, (f) Na, and (g) Zn in 19 temperate tree species ($n = 9$ conifers and $n = 10$ angiosperms) across pyrolysis temperatures of 300, 400, 500, 600, and 700 °C.

Table 1. Species and temperature effect on the variation of nutrient and surface group concentration between conifer and angiosperm species. The values shown are from 19 temperate tree species' biochars ($n = 95$) produced at pyrolysis temperatures of 300, 400, 500, 600, and 700 °C.

Analyte	Species Effect	Temperature Effect	Conifers (mg/Kg)		Angiosperms (mg/Kg)		<i>p</i> -Value
	<i>F</i> -Value	<i>F</i> -Value	Mean	SE	Mean	SE	
Ca	4.9 _{18,73} ***	8.2 _{1,90} **	5888.1	596.1	7294.8	724.4	0.143
K	4.6 _{18,73} ***	5.1 _{1,90} *	1680.1	202.1	3038.8	289.0	<0.001
Mg	6.5 _{18,73} ***	8.1 _{1,90} **	481.2	40.3	766.9	69.8	<0.001
Mn	17.0 _{18,73} ***	4.0 _{1,90} *	317.1	40.2	407.1	64.4	0.239
Fe	2.4 _{18,73} **	4.5 _{1,90} *	90.4	27.7	181.1	22.6	<0.05
Na	7.2 _{18,73} ***	0.3 _{1,90} †	22.4	4.7	61.4	11.4	<0.01
Zn	8.2 _{18,73} ***	1.5 _{1,90} †	31.5	5.3	55.6	9.6	0.030
Carboxylic ‡	0.8 _{18,70} †	150.0 _{1,90} ***	0.153 ‡	0.014	0.247 ‡	0.026	0.002
Lactonic ‡	2.4 _{18,70} **	56.4 _{1,87} ***	0.077 ‡	0.013	0.169 ‡	0.018	<0.05
Phenolic ‡	1.4 _{18,69} †	48.0 _{1,86} ***	0.089 ‡	0.012	0.106 ‡	0.012	0.321

p-values: *** < 0.001, ** < 0.01, * < 0.05, † > 0.05; ‡ units mmol/g; SE = Standard Error.

3.5. Surface Group Analysis

Boehm titration was used to quantify the biochar samples' acidic surface functional groups (carboxylic, lactonic, and phenolic; Figure 3a–c). In all cases, there was a decrease in carboxylic and lactonic functional groups, and an increase in phenolic groups, with increasing pyrolysis temperature. ANOVA results showed significant effects of pyrolysis temperature on carboxylic, lactonic, and phenolic functional group concentrations ($F = 150.0_{1,90}$, $F = 56.4_{1,87}$, and $F = 48.0_{1,86}$, respectively; $p < 0.001$), and showed a significant effect of species on lactonic group concentration only ($F = 2.4_{18,70}$; $p < 0.01$) (Table 1). There was also a consistent difference in the concentrations of surface functional groups between conifers and angiosperms: Angiosperm-derived biochars had overall higher concentrations of carboxylic and lactonic groups, but similar concentrations of phenolic groups (Figure 3a–c).

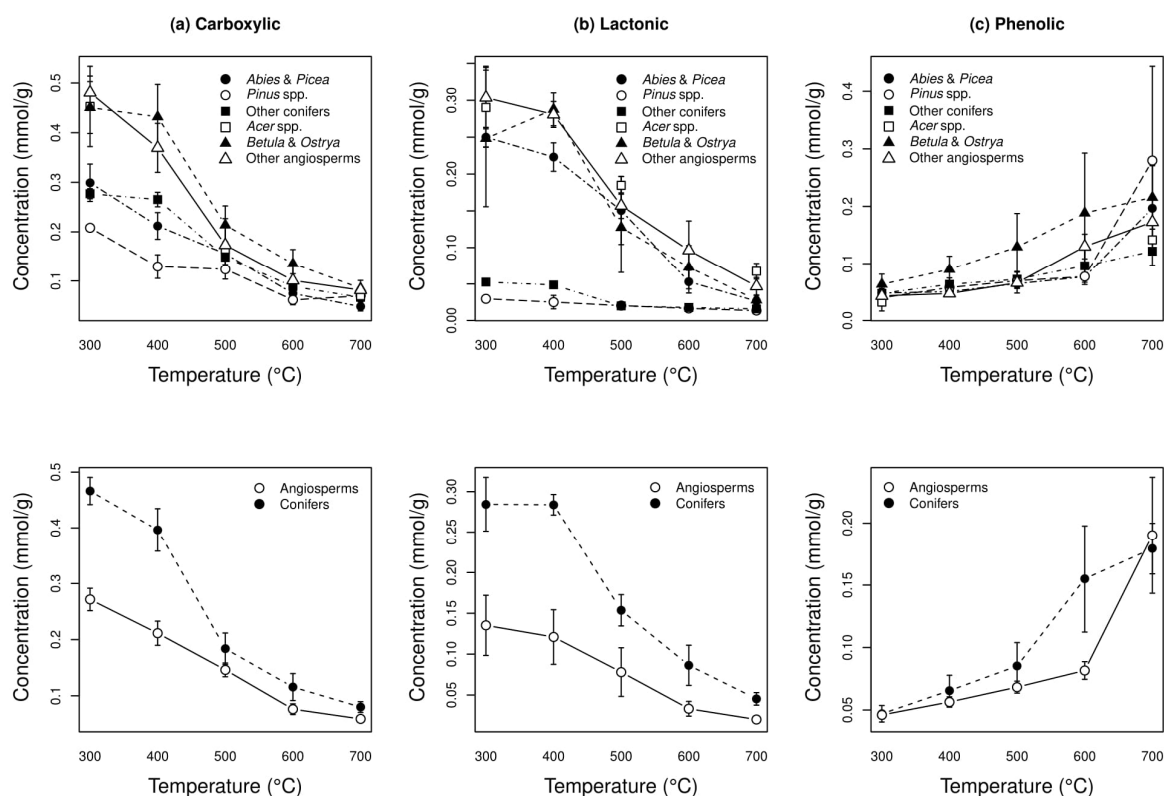


Figure 3. Concentrations of surface functional groups as a function of temperature grouped by six taxonomic groups and grouped by conifers vs. angiosperms: Carboxylic (a), lactonic (b), and phenolic (c), in 19 temperate tree species: Conifer species ($n = 9$) and angiosperm species ($n = 10$).

3.6. FTIR and NMR Spectroscopy

Results obtained from FTIR and NMR spectra further demonstrated the decline of acidic groups and increase of aromatic groups with increasing pyrolysis temperature (Figure 4a). In the FTIR spectrum, biochars produced from 300 to 600 °C exhibited a decrease in relative intensity of the following bands as the temperature increased: 3400 cm^{-1} (O–H stretching of hydroxyl groups), 2900 and 2850 cm^{-1} (C–H asymmetric and symmetric stretching of aliphatic groups), 1620 cm^{-1} (C=O stretching of carboxyl mode), and 1026 cm^{-1} (C–O symmetric stretching of cellulose, hemicellulose, and lignin). Over this same range of pyrolysis temperatures, other bands demonstrated an increase in relative intensity: Specifically, 831 and 700 cm^{-1} (C–H aromatic deformation modes), 1600 cm^{-1} (C=C aromatic stretching and C=O stretching of conjugated ketones and quinones), and 1400 cm^{-1} (C–C stretching of aromatic rings).

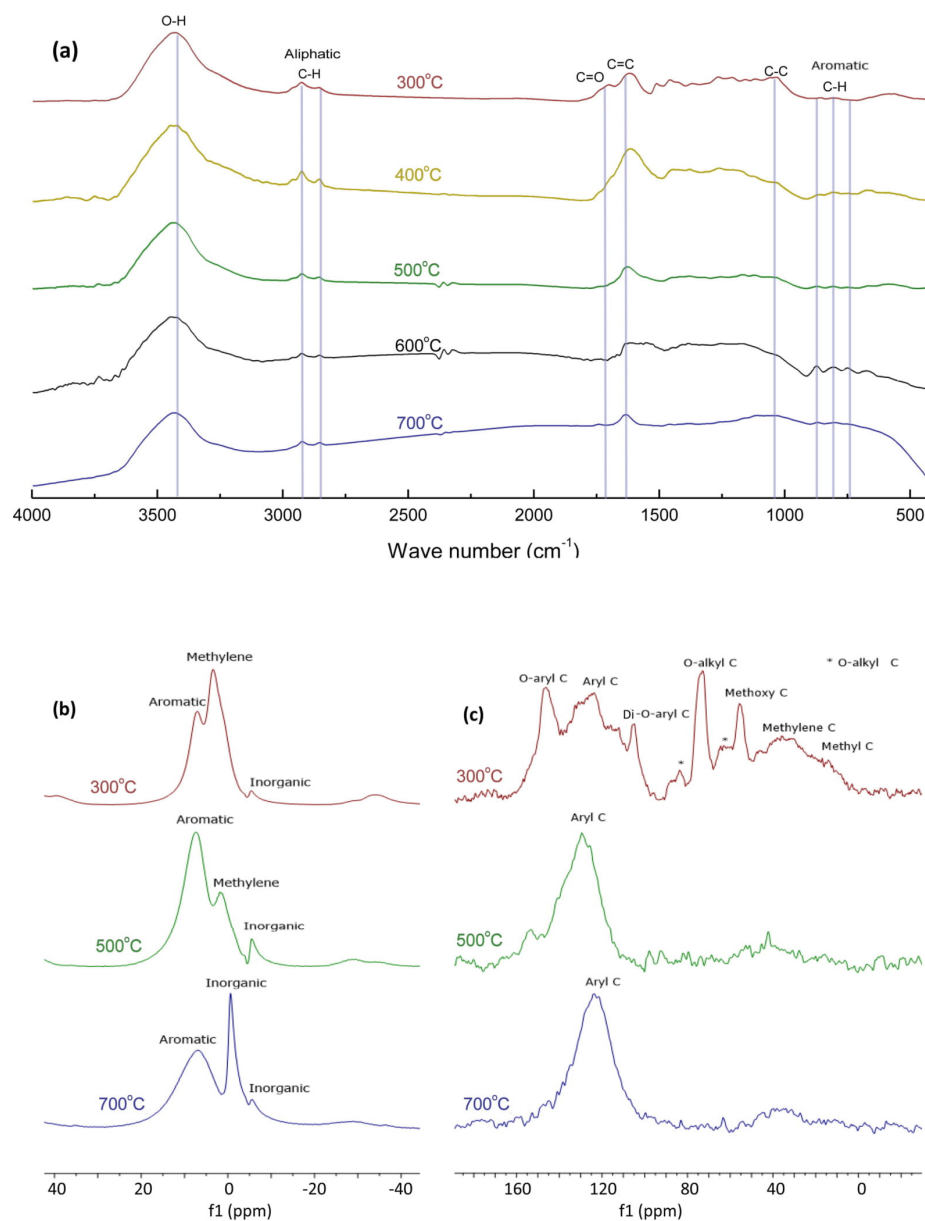


Figure 4. FTIR spectra of *Pinus resinosa* biochars pyrolyzed at 300 to 700 °C pyrolysis temperatures (a); ^1H Nuclear Magnetic Resonance (^1H NMR) (b) and ^{13}C Nuclear Magnetic Resonance (^{13}C NMR) (c) spectra of *Pinus resinosa* biochars pyrolyzed at 300, 500, and 700 °C.

Both ^1H and ^{13}C NMR spectra (Figure 4b,c) detected a decrease in the aliphatic carbons and increase in the aryl carbons. In the ^1H NMR spectrum of biochar prepared at $300\text{ }^\circ\text{C}$, the methylene chemical shift at $\delta = 3.39\text{ ppm}$ decreased in intensity at $500\text{ }^\circ\text{C}$ and disappeared at $700\text{ }^\circ\text{C}$. Aromatic chemical shifts at $\delta = \sim 7\text{ ppm}$ showed increased intensity at $500\text{ }^\circ\text{C}$ and increased broadness at $700\text{ }^\circ\text{C}$. Negative chemical shifts indicate the attachment of inorganic moieties and the high-intensity peak at $700\text{ }^\circ\text{C}$ suggests the presence of carbonates at high concentration. In the ^{13}C NMR spectrum at $300\text{ }^\circ\text{C}$, numerous carbon signals which are related to the feedstock content (cellulose, lignin) and additional chemicals inherited from the feedstock were present. However, at 500 and $700\text{ }^\circ\text{C}$, only aromatic carbons produced signals.

3.7. Modeling the Impact of Element and Surface Group Concentrations on Biochar pH

The acidic surface functional group concentrations of carboxylic, lactonic, and phenolic acid groups (measured in mmol/g), as well as the elemental nutrient concentrations of base metals Ca, Mg, and K (measured in mg/kg), were expected to have an impact on biochar pH. We examined alternative functional forms for this relationship, using a non-linear least-squares method to fit models, and comparing the fit of alternative models based on an information theoretic approach [49] (Table S3). Based on the minimum AIC, the following exponential form best predicted biochar pH as a function of the ratio of carboxylic to phenolic functional groups and concentrations of Ca and K (Equation (1)):

$$\text{pH} = \phi + \alpha (1 - \exp(-\beta \text{ctpr} - \gamma \text{Ca} - \delta \text{K}))$$

where ϕ and α are 6.393 and 3.075; ctpr is the carboxylic to phenolic ratio; Ca and K are the concentrations of Ca and K in mg/kg ; and the fitted coefficients β , γ , and δ are -0.5284 , 1.977×10^{-5} , and 1.496×10^{-5} , respectively. In Figure 5, biochar pH is plotted as a function of the ratio of carboxylic to phenolic groups, with the size of points proportional to summed concentrations of Ca and K. The residual plots for the fitted model are presented in Supplemental Figure S1.

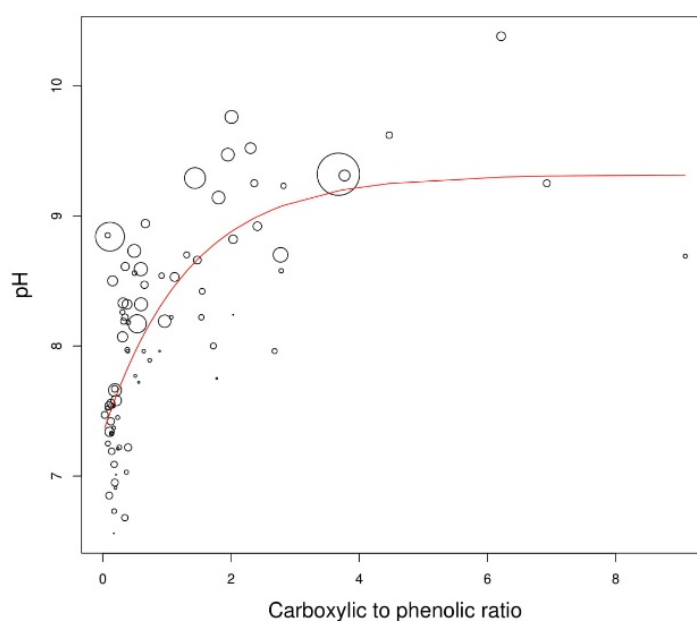


Figure 5. Biochar pH prediction using a non-linear model as a function of char chemistry in 84 slow-pyrolysis wood biochars. The size of points is proportional to the summed concentrations of Ca and K in samples. The fitted equation shown is a non-linear model (Equation (1)), setting Ca and K equal to mean values in the sample.

4. Discussion

Our results indicate that pH of wood-derived biochars is strongly influenced by both pyrolysis temperature and variation in feedstock wood chemistry. Results are also consistent with the predictions that species differences in the temperature dependence of biochar properties are mainly determined by variation in wood chemical composition. The pH of biochars produced at higher pyrolysis temperatures (500–700 °C) is strongly correlated with feedstock pH, while less correlation is observed between the pH of biochars produced at lower temperatures (300–400 °C) and feedstock pH. Correlations between wood feedstock pH and biochar pH indicate that biochar inherits important chemical characteristics from feedstock, and that biochar pH can in part be predicted from feedstock pH. Thermochemical lignocellulose degradation begins at approximately 130 °C, where lignin starts softening; hemicellulose degrades at 150–350 °C, cellulose at 275–350 °C, and lignin at 250–500 °C [18]. The chemical products of hemicellulose degradation are predominantly “wood vinegars” that include a mixture of acetic, propionic, and butyric acids, in addition to other low molecular weight organic acids [51]. Chars can sorb and retain these molecules [51,52]; this is likely to reduce biochar pH in a manner dependent on hemicellulose content and sorption capacity of the char and its non-pyrolyzed constituents. We speculate that the production and sorption of these strongly acidic products may account for the lack of consistent relationships between feedstock and char pH at low pyrolysis temperatures. Possibly, the respective fractions of the wood constituent’s cellulose, hemicellulose, and lignin would show a relationship between feedstock and biochar pH at low pyrolysis temperatures. No prior study has examined relationships between feedstock pH and biochar pH, and, thus, there are no available data to compare to the present results. The overall lower pH of conifer woods and biochars may be influenced by the higher concentration of extractives in conifers, averaging 21% compared to 15%–16% in angiosperms [33,34].

The increase in biochar pH with pyrolysis temperature is accompanied by two parallel patterns: (1) An increasing concentration of basic elements (alkali metals and alkaline earth metals) that are inherited from the feedstock; and (2) a decrease in the concentration of acidic surface functional groups. These results are consistent with prior studies that have found an increase in elements important as plant nutrients [26] and a decrease in acidic functional groups [53] with increasing pyrolysis temperatures. These chemical changes jointly determine biochar pH, which in turn may be used to predict liming capacity. We derive an empirical non-linear expression (Equation (1)) that predicts biochar pH as a function of the ratio of carboxylic to phenolic functional groups and the concentrations of Ca and K in the char.

Elemental analyses indicated that sampled angiosperms had, on average, higher concentrations of Ca, K, Mg, Mn, Fe, Na, and Zn in both feedstocks and in biochars than did conifers (Table 1). This result is consistent with prior surveys of wood chemistry [35], but the generalization of this pattern to chars does not appear to have been previously shown. Our results indicate that biochar pH is most strongly correlated with Ca and K concentration. Studies by Novak et al. [54,55] previously examined biochar’s chemical and physical characteristics, in particular pH, in relation to feedstock and pyrolysis temperature. The Novak et al. [55] study analyzed five different lignocellulosic feedstocks and a poultry litter, finding that as the pyrolysis temperature increased, the biochar’s pH, ash content, and aromaticity increased. This is in agreement with our observations obtained through Boehm titration, FTIR, and NMR spectroscopy. The pine chip char produced by Novak et al. [55] had a lower pH of 6.7 at 500 °C, compared to 7.96 for both *Pinus resinosa* and *Pinus strobus*. Longer pyrolysis residence time increases the concentration of acidic functional groups [56], thus contributing to a decrease in the char’s pH. Other factors such as particle size, N₂ flow, pyrolyzer design, pre- and post-preparation procedures, and conditions of feedstock may also have contributed to the lower pH observed by Novak et al. [55], in addition to effects of condensed volatile matter during pyrolysis. Novak et al. [55] found no relationship between pyrolysis temperature and macronutrient concentrations in wood-derived chars. By contrast, here we observed an increase in mean nutrient concentration with pyrolysis temperature increase across all species and all elements examined, with the exceptions of Na and Zn (Figure 2f,g).

This pattern seems likely to be general at pyrolysis temperatures ranging from 300–700 °C, since higher temperatures dictate a progressive loss of oxygen-containing groups with little volatilization of the nutrient elements in question [57].

Results obtained from the Boehm titration revealed a decrease in carboxylic and lactonic functional groups and an increase in phenolic groups with increasing pyrolysis temperature. This general result is consistent with earlier studies [25,56,58]. Analyses of FTIR and NMR spectra confirmed the results obtained from Boehm titration, showing that aromatic carbons associated with the feedstock biomass increased in concentration with increasing pyrolysis temperature, while the concentration of surface acidic functional groups decreased. The latter result is likewise consistent with previous studies [59,60]. Our observations are novel in that we also observed pronounced variation among wood species in the temperature-dependent changes in oxygen-containing functional groups. Higher concentrations of carboxylic and lactonic groups at a given pyrolysis temperature were generally observed among angiosperms compared to conifers. Biochar pH was negatively correlated with the concentration of carboxylic functional groups, but only weakly to the concentration of lactonic groups, and positively correlated with the concentration of phenolic groups.

Although it has commonly been assumed that more basic biochars will show higher liming capacity, this relationship has not previously been demonstrated. In the present study, all the biochars examined acted to increase soil pH from 5.3 to a range of 7.2–8.0 at a low dosage (0.8% *w/w*). Generally, the highest incubated soil pH was observed at the highest biochar pyrolysis temperatures. The biochar–soil mixture pH increased until it reached equilibrium on Day 18 (Table S2), during which time various chemical reactions could contribute to bringing the biochar pH to equilibrium. The flow chemistry of soluble elements found on biochars varies depending on their chemical composition, temperature, and over time [61], and the leaching mechanisms and amount depend on the biomass type and pyrolysis temperature [62]. For example, at room temperature, water-soluble divalent species of Ca^{2+} and Mg^{2+} have a smaller diffusion coefficient (0.792×10^{-9} and 0.706×10^{-9} m^2/s , respectively) as compared to the monovalent K^+ and Na^+ (1.957×10^{-9} and 1.334×10^{-9} m^2/s , respectively), because the divalent species are bonded more tightly to the biochar, resulting in slower leaching times of divalent ionic species [62,63]. Biochars produced at relatively high temperatures convert their nutrient elements into oxide and carbonate forms, both of which increase biochar alkalinity [64,65]. The water present in the soil–biochar mixture during incubation likely plays an important role in pH equilibrium by reacting with carbonates to form free ions (i.e., Ca^{2+}) [66], and this dissolution of carbonates (e.g., CaCO_3) results in an observed soil pH of between 7.2 and 8.5 [67]. Variable results have been obtained by prior soil incubation studies. Basso [68] observed a pH increase with soil incubation time; however, Novak et al. [69] did not. Basso suggested that the difference in their results occurred due to the ash content difference in biochars: In Basso's case, an increase in the soil pH was mainly attributed to the dissolution of carbonates, oxides, and hydroxides of the biochar ash fraction. Obia et al. [70] also found an increase in pH during incubation, specifically, a 2.3-unit increase upon the application of 1% cacao shell biochar to a sandy loam tropical acrisol soil. Obia et al. [70] suggested that carbonates are a key contributor to the alkalisation effect.

In addition to the effects of basic elements, our results also showed consistently higher pH in both biochar and incubated soil–biochar as carboxylic and lactonic groups decline and phenolic groups increase. Phenolic groups have an aromatic character and are less acidic than carboxylic or lactonic groups. Thus, the increase in concentration of phenolic groups as pyrolysis temperature increases results in higher biochar pH and aromaticity [25]. In conventional batch-leaching systems (in the case of this experiment, soil–biochar cups), acidic species leachate contact with biomass leads to the leaching of some water-insoluble organically bound inorganic species (i.e., Cl and Si) [70]. The inorganic species leaching in a batch condition typically show two-step kinetics: an initial short-period rapid-leaching step followed by a long-period slow-leaching step [62]. Previous studies have noted that in pure water, biochars could also leach some organic matter (i.e., 2–3 and 4–5 aromatic rings) for a period

of up to one month [62,71–73], suggesting that organic matter leaching may also influence incubated soil–biochar pH equilibrium.

In terms of applications, the use of biochar as a soil liming agent will have a “double” effect on climate mitigation by: (1) acting as a long-term C storage in soil and decreasing greenhouse gas emissions [7,74]; and (2) reducing CO₂ emissions from geological liming agents. Application of biochar instead of other liming agents is also beneficial due to the longevity of chars in soil [2], making it possible to omit the frequent application of lime usually required to sustain nutrient availability and exchange capacity [75]. Biochar effects on soil pH in situ may also be affected by long-term weathering processes. The natural oxidation of biochar is believed to enhance phenolic and carboxylic functional groups, thus improving soil ion exchange capacity [25], as suggested by the long-lived fertility of Terra Preta soils [76].

In conclusion, our findings suggest that differences in wood chemistry are reflected in biochar’s liming capacity, which is a central concern for soil amendment applications. Many prior biochar studies do not specify the actual species of wood used, and/or list only broad common names (e.g., “pine”). The differences we document among tree species have important implications for reporting in future biochar studies. Variation in pH and liming capacity of biochars is related to both feedstock and pyrolysis temperature. This work indicates that species differences in wood pH correspond to significant differences in biochar pH and provides a basis for predicting biochar pH from biochar chemistry, and from feedstock pH and pyrolysis temperature. The elevation of pyrolysis temperature corresponds to an increase in elemental nutrient concentrations and a decrease in acidic surface groups, ultimately resulting in an increase in biochar pH. Predicting biochar pH prior to production is of crucial importance because it makes possible the production of application-specific biochars for targeted purposes.

Supplementary Materials: The following are available online at <http://www.mdpi.com/2571-8789/3/2/26/s1>.

Author Contributions: Conceptualization, S.G., M.S. and S.C.T.; Methodology, S.G., M.S. and S.C.T.; Formal Analysis, S.G. and S.C.T.; Investigation, S.G.; Resources, M.S. and S.C.T.; Writing-Original Draft Preparation, S.G.; Writing-Review & Editing, S.G. and S.C.T.; Supervision, M.S. and S.C.T.; Funding Acquisition, M.S. and S.C.T.

Funding: This research was funded by grants from the Natural Sciences and Engineering and Research Council of Canada, ORF-RE, TOTAL NA, and Ford Motor Company.

Acknowledgments: We thank Haliburton Forest and Wildlife Reserve Ltd. for support and provision of materials, and Christine LeDuc for assistance with collection of feedstock samples. We are also grateful to Katerina Eyre, Maria Al Zayat, Aidan Wischnowski and Jad Murtada for assisting in soil incubation experiments. Special thanks to Lutchmee Sujeeun for assisting in several laboratory tasks.

Conflicts of Interest: The authors declare no conflict of interest. The funding sponsors had no role in the design of the study; in the collection, analyses, or interpretation of data; in the writing of the manuscript, or in the decision to publish the results.

References

1. Lehmann, J.; Joseph, S. *Biochar for Environmental Management: Science, Technology and Implementation*, 2nd ed.; Earthscan: London, UK, 2015; pp. 3–71.
2. Spokas, K.A. Review of the stability of biochar in soils: Predictability of O:C molar ratios. *Carbon Manag.* **2010**, *1*, 289–303. [[CrossRef](#)]
3. Lehmann, J.; da Silva, J.P., Jr.; Steiner, C.; Nehls, T.; Zech, W.; Glaser, B. Nutrient availability and leaching in an archaeological Anthrosol and a Ferralsol of the Central Amazon basin: Fertilizer, manure and charcoal amendments. *Plant Soil* **2010**, *249*, 343–357. [[CrossRef](#)]
4. Inguanzo, M.; Domínguez, A.; Menéndez, J.A.; Blanco, C.G.; Pis, J.J. On the pyrolysis of sewage sludge: The influence of pyrolysis conditions on solid, liquid and gas fractions. *J. Anal. Appl. Pyrol.* **2002**, *63*, 209–222. [[CrossRef](#)]
5. Cantrell, K.; Ro, K.; Mahajan, D.; Anjom, M.; Hunt, P.G. Role of thermochemical conversion in livestock waste-to-energy treatments: Obstacles and opportunities. *Ind. Eng. Chem. Res.* **2007**, *46*, 8918–8927. [[CrossRef](#)]

6. Spokas, K.A.; Cantrell, K.B.; Novak, J.M.; Archer, D.W.; Ippolito, J.A.; Collins, H.P.; Boateng, A.A.; Lima, I.M.; Lamb, M.C.; McAloon, A.J.; Lentz, R.D.; Nichols, K.A. Biochar: A synthesis of its agronomic impact beyond carbon sequestration. *J. Env. Qual.* **2012**, *41*, 973–989. [[CrossRef](#)] [[PubMed](#)]
7. Ippolito, J.A.; Laird, D.A.; Busscher, W.J. Environmental benefits of biochar. *J. Env. Qual.* **2012**, *41*, 967–972. [[CrossRef](#)]
8. Ekpete, O.A.; Horsfall, M.J.N.R. Preparation and characterization of activated carbon derived from fluted pumpkin stem waste (*Telfairia occidentalis* Hook F). *Res. J. Chem. Sci.* **2011**, *1*, 10–17.
9. Qadeer, R.; Hanif, J.; Saleem, M.; Afzal, M. Characterization of activated charcoal. *J. Chem. Soc. Pak.* **1994**, *16*, 229–235.
10. Liu, Y.; He, Z.; Uchimiya, M. Comparison of biochar formation from various agricultural by-products using FTIR spectroscopy. *Mod. Appl. Sci.* **2014**, *9*, 246–253. [[CrossRef](#)]
11. Emmerich, F.G.; de Sousa, J.C.; Torriani, I.L.; Luengo, C.A. Applications of a granular model and percolation theory to the electrical resistivity of heat treated endocarp of babassu nut. *Carbon* **1987**, *25*, 417–424. [[CrossRef](#)]
12. Chia, C.H.; Downie, A.; Munroe, P. Characteristics of biochar: Physical and structural properties. In *Biochar for Environmental Management: Science, Technology and Implementation*, 2nd ed.; Lehmann, J., Joseph, S., Eds.; Earthscan: London, UK, 2015; pp. 89–109.
13. Vassilev, N.; Martos, E.; Mendes, G.; Martos, V.; Vassileva, M. Biochar of animal origin: A sustainable solution to the global problem of high-grade rock phosphate scarcity? *J. Sci. Food Agric.* **2013**, *93*, 1799–1804. [[CrossRef](#)]
14. Kloss, S.; Zehetner, F.; Dellantonio, A.; Hamid, R.; Ottner, F.; Liedtke, V.; Schwanninger, M.; Gerzabek, M.H.; Soja, G. Characterization of slow pyrolysis biochars: Effects of feedstocks and pyrolysis temperature on biochar properties. *J. Env. Qual.* **2012**, *41*, 990. [[CrossRef](#)] [[PubMed](#)]
15. Lehmann, J. Bio-energy in the black. *Front. Ecol. Env.* **2007**, *5*, 381–387. [[CrossRef](#)]
16. Peng, X.Y.; Ye, L.L.; Wang, C.H.; Zhou, H.; Sun, B. Temperature- and duration-dependent rice straw-derived biochar: Characteristics and its effects on soil properties of an ultisol in southern China. *Soil Tillage Res.* **2011**, *112*, 159–166. [[CrossRef](#)]
17. Lua, A.C.; Yang, T.; Guo, J. Effects of pyrolysis conditions on the properties of activated carbons prepared from pistachio-nut shells. *J. Anal. Appl. Pyrol.* **2004**, *72*, 279–287. [[CrossRef](#)]
18. Basu, P. *Biomass Gasification and Pyrolysis*; Academic Press: Burlington, MA, USA, 2010.
19. Demirbas, A. Effects of temperature and particle size on bio-char yield from pyrolysis of agricultural residues. *J. Anal. Appl. Pyrol.* **2004**, *72*, 243–248. [[CrossRef](#)]
20. Beesley, L.; Moreno-Jiménez, E.; Gomez-Eyles, J.L.; Harris, E.; Robinson, B.; Sizmur, T. A review of biochars' potential role in the remediation, revegetation and restoration of contaminated soils. *Env. Pollut.* **2011**, *159*, 3269–3282. [[CrossRef](#)] [[PubMed](#)]
21. Wang, T.; Camps-Arbestain, M.; Hedley, M.; Singh, B.P.; Calvero-Pereira, R.; Wang, C. Determination of carbonate-C in biochars. *Soil Res.* **2014**, *52*, 495–504. [[CrossRef](#)]
22. Liu, X.; Zhang, A.; Ji, C.; Joseph, S.; Bian, R.; Li, L.; Pan, G.; Paz-Ferreiro, J. Biochar's effect on crop productivity and the dependence on experimental conditions—a meta-analysis of literature data. *Plant Soil* **2013**, *373*, 583–594. [[CrossRef](#)]
23. Gomez-Eyles, J.L.; Sizmur, T.; Collins, C.D.; Hodson, M.E. Effects of biochar and the earthworm *Eisenia fetida* on the bioavailability of polycyclic aromatic hydrocarbons and potentially toxic elements. *Env. Pollut.* **2011**, *159*, 616–622. [[CrossRef](#)]
24. Rees, F.; Simonnot, M.O.; Morel, J.L. Short-term effects of biochar on soil heavy metal mobility are controlled by intra-particle diffusion and soil pH increase. *Eur. J. Soil Sci.* **2014**, *65*, 149–161. [[CrossRef](#)]
25. Mukherjee, A.; Zimmerman, A.R.; Harris, W. Surface chemistry variations among a series of laboratory-produced biochars. *Geoderma* **2011**, *163*, 247–255. [[CrossRef](#)]
26. Van Zwieten, L.; Kimber, S.; Morris, S.; Chan, K.Y.; Downie, A.; Rust, J.; Joseph, S.; Cowie, A. Effects of biochar from slow pyrolysis of papermill waste on agronomic performance and soil fertility. *Plant Soil* **2009**, *327*, 235–246. [[CrossRef](#)]
27. Wei, L.; Xu, G.; Shao, H.; Sun, J.; Chang, S.X. Regulating environmental factors of nutrients release from wheat straw biochar for sustainable agriculture. *Clean Soil Air Water* **2013**, *41*, 697–701. [[CrossRef](#)]

28. Lai, W.; Lai, C.-M.; Ke, G.-R.; Chung, R.-S.; Chen, C.-T.; Cheng, C.-H.; Pai, C.-W.; Chen, S.-Y.; Chen, C.-C. The effects of woodchip biochar application on crop yield, carbon sequestration and greenhouse gas emissions from soils planted with rice or leaf beet. *J. Taiwan Inst. Chem. Eng.* **2013**, *44*, 1039–1044. [[CrossRef](#)]
29. Sackett, T.E.; Basiliko, N.; Noyce, G.L.; Winsborough, C.; Schurman, J.; Ikeda, C.; Thomas, S.C. Soil and greenhouse gas responses to biochar additions in a temperate hardwood forest. *GCB Bioenergy* **2015**, *7*, 1062–1074. [[CrossRef](#)]
30. Thomas, S.C.; Gale, N. Biochar and forest restoration: A review and meta-analysis of tree growth responses. *New For.* **2015**, *46*, 931–946. [[CrossRef](#)]
31. Glaser, B.; Lehmann, J.; Zech, W. Ameliorating physical and chemical properties of highly weathered soils in the tropics with charcoal—A review. *Biol. Fertil. Soils* **2002**, *35*, 219–230. [[CrossRef](#)]
32. Cheng, C.-H.; Lehmann, J.; Thies, J.E.; Burton, S.D.; Engelhard, M.H. Oxidation of black carbon by biotic and abiotic processes. *Org. Geochem.* **2006**, *37*, 1477–1488. [[CrossRef](#)]
33. Pettersen, R.C. The chemical composition of wood. In *The Chemistry of Solid Wood*; Rowell, R., Ed.; American Chemical Society: Washington, DC, USA, 1984; Volume 207, pp. 57–126.
34. Rowell, R.M. *Handbook of Wood Chemistry and Wood Composites*; CRC Press: Boca Raton, FL, USA, 2005; pp. 34–48.
35. Meerts, P. Mineral nutrient concentrations in sapwood and heartwood: A literature review. *Ann. Sci.* **2002**, *59*, 713–722. [[CrossRef](#)]
36. Pluchon, N.; Casetou, S.C.; Kardol, P.; Gundale, M.J.; Nilsson, M.-C.; Wardle, D.A. Influence of species identity and charring conditions on fire-derived charcoal traits. *Can. J. Res.* **2015**, *45*, 1669–1675. [[CrossRef](#)]
37. Abdel-Fattah, T.M.; Mahmoud, M.E.; Ahmed, S.B.; Huff, M.D.; Lee, J.W.; Kumar, S. Biochar from woody biomass for removing metal contaminants and carbon sequestration. *J. Korean Ind. Eng. Chem.* **2015**, *22*, 103–109. [[CrossRef](#)]
38. Xie, X.; Goodell, B.; Zhang, D.; Nagle, D.C.; Qian, Y.; Peterson, M.L.; Jellison, J. Characterization of carbons derived from cellulose and lignin and their oxidative behavior. *Bioresour. Technol.* **2009**, *100*, 1797–1802. [[CrossRef](#)] [[PubMed](#)]
39. Müller-Hagedorn, M.; Bockhorn, H.; Krebs, L.; Müller, U. A comparative kinetic study on the pyrolysis of three different wood species. *J. Anal. Appl. Pyrol.* **2003**, *68–69*, 231–249. [[CrossRef](#)]
40. Mohan, D.; Pittman, C.U.; Steele, P.H. Pyrolysis of wood/biomass for bio-oil: A critical review. *Energy Fuels* **2006**, *20*, 848–889. [[CrossRef](#)]
41. Afifi, A.I.; Chornet, E.; Overend, R.P.; Hindermann, J.P. The upgrading of lignin-derived compounds: Case studies on model compounds. In *Research in Thermochemical Biomass Conversion*; Bridgwater, A., Kuester, J., Eds.; Springer: Dordrecht, The Netherlands, 1988; pp. 439–451.
42. Thomas, S.C. Biochar and its potential in Canadian forestry. *Silvic. Mag.* **2013**, 4–6.
43. Mansfield, S.D.; Weineisen, H. Wood fiber quality and kraft pulping efficiencies of trembling aspen (*Populus tremuloides Michx*) clones. *J. Wood Chem. Technol.* **2007**, *27*, 135–151. [[CrossRef](#)]
44. Heschel, H.; Klose, E. On the suitability of agricultural by-products for the manufacture of granular activated carbon. *Fuel* **1995**, *74*, 1786–1791. [[CrossRef](#)]
45. Fidel, R.B.; Laird, D.A.; Thompson, M.L. Evaluation of modified Boehm titration methods for use with biochars. *J. Env. Qual.* **2013**, *42*, 1771–1778. [[CrossRef](#)]
46. Goertzen, S.L.; Thériault, K.D.; Oickle, A.M.; Tarasuk, A.C.; Andreas, H.A. Standardization of the Boehm titration: Part I. CO₂ expulsion and endpoint determination. *Carbon* **2010**, *48*, 1252–1261. [[CrossRef](#)]
47. Enders, A.; Lehmann, J. Comparison of wet-digestion and dry-ashing methods for total elemental analysis of biochar. *Commun. Soil Sci. Plant Anal.* **2012**, *43*, 1042–1052. [[CrossRef](#)]
48. McDonald, J.H. *Handbook of Biological Statistics*, 3rd ed.; Sparky House: Baltimore, MA, USA, 2013; pp. 4–6.
49. Burnham, K.P.; Anderson, D.R. *Model Selection and Multimodel Inference: A Practical Information-Theoretic Approach*, 2nd ed.; Springer-Verlag: New York, NY, USA, 2002.
50. R Core Team. *R: A Language and Environment for Statistical Computing*; R Foundation for Statistical Computing: Vienna, Austria, 2014.
51. Spokas, K.A.; Novak, J.M.; Stewart, C.E.; Cantrell, K.B.; Uchimiya, M.; DuSaire, M.G.; Ro, K.S. Qualitative analysis of volatile organic compounds on biochar. *Chemosphere* **2011**, *85*, 869–882. [[CrossRef](#)]
52. Gale, N.V.; Sackett, T.E.; Thomas, S.C. Thermal treatment and leaching of biochar alleviates plant growth inhibition from mobile organic compounds. *PeerJ* **2016**, *4*, e2385. [[CrossRef](#)] [[PubMed](#)]

53. Ronsse, F.; van Hecke, S.; Dickinson, D.; Prins, W. Production and characterization of slow pyrolysis biochar: Influence of feedstock type and pyrolysis conditions. *GCB Bioenergy* **2013**, *5*, 104–115. [[CrossRef](#)]
54. Novak, J.M.; Lima, I.; Xing, B.; Gaskin, J.W.; Steiner, C.; Das, K.C.; Ahmedna, M.; Rehrh, D.; Watts, D.W.; Busscher, W.J.; Schomberg, H. Characterization of designer biochar produced at different temperatures and their effects on a loamy sand. *Ann. Env. Sci.* **2009**, *3*, 195–206.
55. Novak, J.M.; Cantrell, K.B.; Watts, D.W. Compositional and thermal evaluation of lignocellulosic and poultry litter chars via high and low temperature pyrolysis. *Bioenergy Res.* **2012**, *6*, 114–130. [[CrossRef](#)]
56. Rutherford, D.W.; Wershaw, R.L.; Reeves, J.B., III. Development of acid functional groups and lactones during the thermal degradation of wood and wood components. In *US Geological Survey Scientific Investigations Report 2007–5013*; U.S. Geological Survey: Reston, VA, USA, 2008.
57. Enders, A.; Hanley, K.; Whitman, T.; Joseph, J.; Lehmann, J. Characterization of biochars to evaluate recalcitrance and agronomic performance. *Bioresour. Technol.* **2012**, *114*, 644–653. [[CrossRef](#)] [[PubMed](#)]
58. Han, Y.; Boateng, A.A.; Qi, P.X.; Lima, I.M.; Chang, J. Heavy metal and phenol adsorptive properties of biochars from pyrolyzed switchgrass and woody biomass in correlation with surface properties. *J. Env. Manag.* **2013**, *118*, 196–204. [[CrossRef](#)]
59. Reeves III, J.B. Mid-infrared spectroscopy of biochars and spectral similarities to coal and kerogens: What are the implications? *Appl. Spectrosc.* **2012**, *66*, 689–695. [[CrossRef](#)]
60. Brewer, C.E.; Hu, Y.-Y.; Schmidt-Rohr, K.; Loynachan, T.E.; Laird, D.A.; Brown, R.C. Extent of pyrolysis impacts on fast pyrolysis biochar properties. *J. Env. Qual.* **2012**, *41*, 1115–1122. [[CrossRef](#)]
61. Reid, W.T. The relation of mineral composition to slagging, fouling and erosion during and after combustion. *Prog. Energy Combust. Sci.* **1984**, *10*, 159–169. [[CrossRef](#)]
62. Liaw, S.B.; Wu, H. Leaching characteristics of organic and inorganic matter from biomass by water: Differences between batch and semi-continuous operations. *Ind. Eng. Chem. Res.* **2013**, *52*, 4280–4289. [[CrossRef](#)]
63. Weast, R.C.; Astle, M.J.; Beyer, W.H. *CRC Handbook of Chemistry and Physics*, 66th ed.; CRC Press: Boca Raton, FL, USA, 1986.
64. Berek, A.K.; Hue, N.V. Characterization of biochars and their use as an amendment to acid soils. *Soil Sci.* **2016**, *181*, 412–426. [[CrossRef](#)]
65. Singh, B.; Singh, B.P.; Cowie, A.L. Characterization and evaluation of biochars for their application as a soil amendment. *Aust. J. Soil Res.* **2010**, *48*, 516–525. [[CrossRef](#)]
66. Karberg, N.J.; Pregitzer, K.S.; King, J.S.; Friend, A.L.; Wood, J.R. Soil carbon dioxide partial pressure and dissolved inorganic carbonate chemistry under elevated carbon dioxide and ozone. *Oecologia* **2005**, *142*, 296–306. [[CrossRef](#)] [[PubMed](#)]
67. Sawyer, J. Soil pH and Liming. Presented at the Soil Fertility and Nutrient Management Short Course, Iowa State University, Ames, IA, USA, 2004. Available online: <http://www.agronext.iastate.edu/soilfertility/info/SoilpHandLiming2017.pdf> (accessed on 1 April 2019).
68. Basso, A.S. Effect of fast pyrolysis biochar on physical and chemical properties of a sandy soil. Master's Thesis, Iowa State University, Ames, IA, USA, 2012. [[CrossRef](#)]
69. Novak, J.M.; Busscher, W.J.; Laird, D.; Ahmedna, M.; Watts, D.W.; Niandou, M.A.S. Impact of biochar amendment on fertility of a southeastern coastal plain soil. *Soil Sci.* **2009**, *174*, 105–112. [[CrossRef](#)]
70. Obia, A.; Cornelissen, G.; Mulder, J.; Dörsch, P. Effect of soil pH increase by biochar on NO, N₂O and N₂ production during denitrification in acid soils. *PLoS ONE* **2015**, *10*, e0138781. [[CrossRef](#)]
71. Keown, D.M.; Favas, G.; Hayashi, J.; Li, C.Z. Volatilization of alkali and alkaline earth metallic species during the pyrolysis of biomass: Differences between sugar cane bagasse and cane trash. *Bioresour. Technol.* **2005**, *96*, 1570–1577. [[CrossRef](#)]
72. Wu, H.; Yip, K.; Kong, Z.; Li, C.Z.; Liu, D.; Yu, Y.; Gao, X. Removal and recycling of inherent inorganic nutrient species in Mallee biomass and derived biochars by water leaching. *Ind. Eng. Chem. Res.* **2011**, *50*, 12143–12151. [[CrossRef](#)]
73. Lievens, C.; Mourant, D.; Gunawan, R.; Hu, X.; Wang, Y. Organic compounds leached from fast pyrolysis mallee leaf and bark biochars. *Chemosphere* **2015**, *139*, 659–664. [[CrossRef](#)]
74. Ubando, A.T.; Culaba, A.B.; Aviso, K.B.; Ng, D.K.S.; Tan, R.R. Fuzzy mixed-integer linear programming model for optimizing a multi-functional bioenergy system with biochar production for negative carbon emissions. *Clean Technol. Env. Policy* **2014**, *16*, 1537–1549. [[CrossRef](#)]

75. Lukin, V.V.; Epplin, F.M. Optimal frequency and quantity of agricultural lime applications. *Agr. Syst.* **2003**, *76*, 949–967. [[CrossRef](#)]
76. Lima, H.N.; Schaefer, C.E.R.; Mello, J.W.V.; Gilkes, R.J.; Ker, J.C. Pedogenesis and pre-Colombian land use of “Terra Preta Anthrosols” (“Indian black earth”) of Western Amazonia. *Geoderma* **2002**, *110*, 1–17. [[CrossRef](#)]



© 2019 by the authors. Licensee MDPI, Basel, Switzerland. This article is an open access article distributed under the terms and conditions of the Creative Commons Attribution (CC BY) license (<http://creativecommons.org/licenses/by/4.0/>).